Open access • Journal Article • DOI:10.1029/2021GL093127

No Cryosphere-Confined Aquifer Below InSight on Mars — Source link

Michael Manga, Vanshan Wright

Institutions: University of California, Berkeley, Woods Hole Oceanographic Institution

Published on: 28 Apr 2021 - Geophysical Research Letters (John Wiley & Sons, Ltd)

Topics: Aquifer, Martian, Seismometer, Mars Exploration Program and Crust

Title
No Cryosphere-Confined Aquifer Below InSight on Mars

Journal
Geophysical Research Letters, 48(8)

ISSN
0094-8276

Authors
Manga, M
Wright, V

Publication Date
2021-04-28

DOI
10.1029/2021GL093127

Peer reviewed

Geophysical Research Letters

RESEARCH LETTER
10.1029/2021GL093127

Key Points:

- We interpret the seismic wave velocity of the Martian crust measured by InSight
- We quantity the effects of ice and water on seismic velocity using a rock physics model
- Measurements preclude a layer of ice-filled crust that confines liquid water in an aquifer

Correspondence to:
M. Manga,
manga@seismo.berkeley.edu

Citation:
Manga, M., & Wright, V. (2021). No cryosphere-confined aquifer below InSight on Mars. *Geophysical Research Letters*, *48*, e2021GL093127. https://doi.org/10.1029/2021GL093127

Received 24 FEB 2021
Accepted 2 APR 2021

No Cryosphere-Confined Aquifer Below InSight on Mars

Michael Manga[1] **and Vanshan Wright**[2]

[1]Department of Earth and Planetary Science, University of California Berkeley, Berkeley, CA, USA, [2]Geology and Geophysics Department, Woods Hole Oceanographic Institution, MA, USA

Abstract The seismometer deployed by the InSight lander measured the seismic velocity of the Martian crust. We use a rock physics model to interpret those velocities and constrain hydrogeological properties. The seismic velocity of the upper ~10 km is too low to be ice-saturated. Hence there is no cryosphere that confines deeper aquifers and possibly no aquifers locally. An increase in seismic velocity at depths of ~10 km could be explained by a few volume percent of mineral cement (1%–5%) in pore space and may document the past depth of aquifers.

Plain Language Summary Large amounts of water may be stored in the Martian crust and episodically released to flood the surface. Where this water exists, and even why, is uncertain. The seismometer on the InSight lander measured the velocity of seismic waves in the Martian crust. The presence of ice and water affects seismic velocity. We argue that the measurements preclude a layer of ice-filled crust that confines liquid water in an aquifer.

1. Introduction

Large volumes of water are hypothesized to have carved and passed through the Martian outflow channels (e.g., Baker, 2001). Because these channels originate from discrete sources, a groundwater origin is typically invoked (e.g., Head et al., 2003). Given the large discharges needed to create the observed landforms, in some cases a couple orders of magnitude greater than the largest catastrophic floods on Earth (Baker, 1982), large and permeable aquifers would be needed (e.g., Carr, 1979; Manga, 2004). While most of the outflow channels are Hesperian (e.g., Tanaka, 1997), their formation continued through the Amazonian (e.g., Rodriguez et al., 2015). Some of the youngest channels originated from fissures in Athabasca Valles, Eastern Elysium Planitia within the past 10s of millions of years (Burr et al., 2002; Voigt & Hamilton, 2018). The subsurface of Mars thus appears to have hosted and episodically released large volumes of water over most of Martian history. Hence, detecting the presence and quantifying the volume of subsurface water and ice would help constrain the water budget and cycle from the Noachian to present (e.g., Clifford and Parker, 2001), the amount of water lost to space (e.g., Jakosky, 2021), the fate of possible oceans (e.g., Citron et al., 2018), and the amount of water sequestered in minerals (e.g., Scheller et al., 2021).

To discharge water at the surface, aquifers must have sufficient pressure for water to reach the surface. One way to achieve hydraulic heads greater than hydrostatic and hence enable surface discharge is to confine aquifers beneath an overlying ice-saturated crust or cryosphere (e.g., Andrews-Hanna and Phillips, 2007; Carr, 1996; Harrison & Grimm, 2004). As Mars cools and this cryosphere thickens, hydraulic heads will increase and may also create the pressure needed to fracture the crust (Wang et al., 2006). The MARSIS radar system has identified reflections interpreted as lakes confined under Mars' southern ice cap (Lauro et al., 2021; Orosei et al., 2018), though this interpretation is contested (Ojha et al., 2021) and would require recent magmatism (Sori & Bramson, 2019). Aquifers in the crust, if they exist, would be at depths of several kilometers (Clifford et al., 2010), deeper than the MARSIS and SHARAD radar systems can penetrate in volcanic terrain (e.g., Abotalib & Heggy, 2019). MARSIS has not identified a deep reflector indicative of an aquifer below the outflow channels in Athabasca Valles, for example (Clifford et al., 2010). Other geophysical data, such as seismic shear wave velocity, Vs, may be useful because Vs is sensitive to physical properties of the subsurface and probes greater depths.

Our objective is to interpret Vs measured by the InSight mission in Elysium Planitia. We use rock physics models to compute effective medium properties and to help distinguish between porous basalt filled with gas, liquid water, ice, or mineral cement. We focus on two observations. First, Vs within Mars' upper

Table 1
Properties of Materials in the Martian Crust That Affect Seismic Velocity (From Heap, 2019)

	Density (kg/m^3)	Bulk modulus K (Pa)	Shear modulus μ (Pa)
Basalt solids	2,900	8.0×10^{10}	4.0×10^{10}
Liquid water	1,000	2.2×10^{9}	0
Water ice	910	8.1×10^{9}	3.7×10^{9}
Gas	1.8	1.0×10^{5}	0

~8–11 km is ~1.7–2.1 km/s (Lognonné et al., 2020) and possibly lower (Knapmeyer-Endrun et al., 2020). Lognonné et al. (2020) attribute these relatively low Vs to "highly altered and or damaged layers." Second, receiver function analyses suggest that Vs increases by ~0.4–1 km/s below depths of ~8–11 km (Figure S4-9c in Lognonné et al., 2020).

2. Model

We constrain Mars' subsurface hydrology by comparing Vs computed from InSight seismometer data with Vs modeled for gas, liquid water, and ice-filled porous basalt. We estimate Vs from the effective elastic moduli (bulk and shear moduli) and bulk density of basalt. In the absence of information on the nature of the actual pore space, we model the pore space with randomly oriented oblate ellipsoidal inclusions with specified aspect ratios. We compute effective elastic moduli with a so-called self-consistent approximation based on the elastic deformation of single inclusion embedded in a background medium with the elastic properties of the effective medium. For gas and ice-saturated pores, for the shear modulus μ and bulk modulus K, we use the Wu (1966) self-consistent (subscript SC) moduli estimates for two-phase composites

$$\mu^*_{SC} = \mu_m + \phi\left(\mu_i - \mu_m\right)Q^* \tag{1}$$

and

$$K^*_{SC} = K_m + \phi\left(K_i - K_m\right)P^* \tag{2}$$

where i and m represent inclusion and matrix values, * represents effective medium values, and ϕ is the volume fraction of inclusions. Q and P are geometric shape factors for the inclusion that characterize the effect of inclusion shape and material properties, and depend on μ^*_{SC} and K^*_{SC} (Berryman, 1980). Aspect ratio is the minor axis divided by the major axis; more elongate pores have smaller aspect ratios. Equations 1 and 2 are coupled and hence are solved by simultaneous iteration. Bulk density is based on the volume-weighted average,

$$\rho^* = \left(1 - \phi\right)\rho_m + \phi\rho_i. \tag{3}$$

Vs is then computed by

$$\text{Vs} = \sqrt{\frac{\mu^*_{SC}}{\rho^*}}. \tag{4}$$

We estimate Vs for water-filled pores by using Gassmann-Biot theory to saturate dry inclusions (page 169 of Mavko et al., 1998). This is appropriate for frequencies <100 Hz, and hence the frequency of seismic waves on Mars, where there is no relative motion between fluids and solids and thus no frequency-dependence of Vs.

We use elastic moduli and bulk densities for basalt compiled in Heap (2019), summarized in Table 1. We choose basalt for the solid phase because it should dominate the subsurface beneath InSight (Golombek et al., 2020). Vacuum versus gas-filled pores will have negligible effects on results and conclusions because gas density is significantly lower than basalt and liquid water densities, and gas compressibility is significantly greater than the compressibility of basalt and liquid water.

3. Results

We consider porosities ($=100 \times \phi$) up to 30% and pore aspect ratios from 0.03 to 1. For ice-saturated basalt, Vs is always intermediate between that of ice and solid basalt, and Vs is always greater than 2.6 km/s (Figure 1). Increasing porosity and pore oblateness both decrease velocity. Replacing the ice with gas lowers Vs

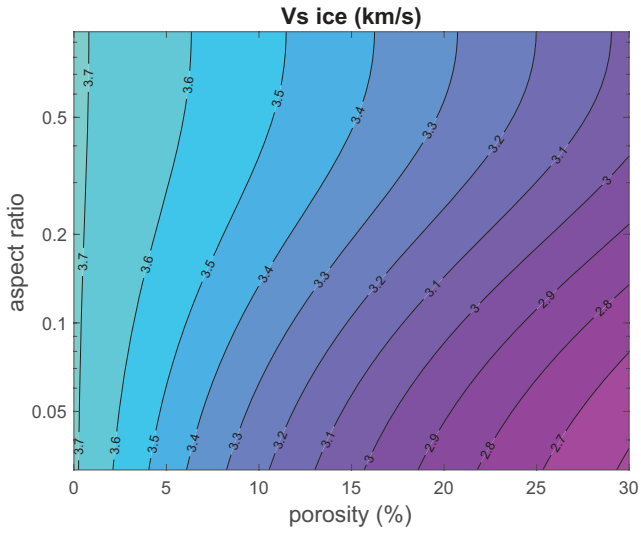

Figure 1. S wave velocity shear wave velocity (Vs) (contours in km/s) for ice-filled ellipsoidal pores as a function of aspect ratio and porosity. All these velocities exceed that of the upper 8–11 km of the Martian crust.

by lowering shear modulus more than bulk density (Figure 2). Because water and gas shear moduli are zero, and water is denser than gas, replacing gas with water decreases Vs. In passing from a gas-to water-saturated crust, we should thus expect Vs to decrease a small amount, assuming that the pores do not change (Figure 3).

4. Discussion

Uncertainties in measured Vs and approximations inherent in the model guide our interpretations. There are uncertainties in the magnitude of Vs, the depth of changes, and the sharpness of Vs-depth change (Lognonné et al., 2020). The rock physics model is idealized, though it can reproduce measured Vs-porosity relationships in Earth basalts (e.g., Heap, 2019). Natural sedimentary and igneous rocks beneath the InSight lander likely contain multiple pore structures ranging from fractures to intergranular pores in sediments and vesicles in volcanic rocks. In the absence of detailed information about subsurface lithology and velocity-depth profiles (e.g., borehole vertical seismic profiling velocities), we represent the subsurface with a homogeneous, isotropic porous material. With these limitations in mind, we focus on the most robust inferences that should not be sensitive to uncertain details in the observations and idealizations in the model.

4.1. No Thick, Ice-Saturated Cryosphere

Vs of 1.7–2.1 km/s in the upper 8–11 km of the crust beneath Insight (Lognonné et al., 2020) is similar to or lower than standard pure ice Vs (2.0 km/s) (Gagnon et al., 1988). No rock physics modeling is thus needed to conclude that the low measured velocities are incompatible with an ice-saturated regolith or crust. Predicted ice-filled Vs (Figure 1) is also much larger than observed Vs, even for high porosity (30%) and very elongated (aspect ratio = 0.03) pores.

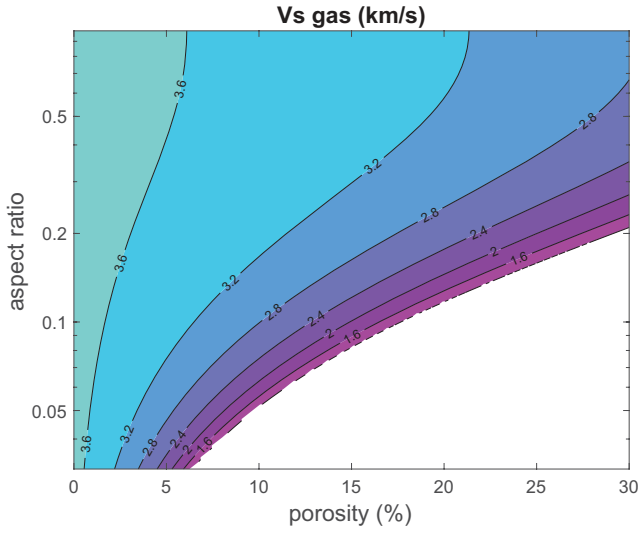

Figure 2. S wave velocity shear wave velocity (Vs) (contours in km/s) for gas-filled ellipsoidal pores as a function of aspect ratio and porosity. White shows regions where the Wu (1966) model leads to unphysical velocities as approximations break down.

Patchy ice saturation may be possible–adding some ice will lead to velocities intermediate between those shown for dry and ice-saturated materials (Figures 1 and 2). If the water is briny owing to weathering and evaporation, a brine + ice mixture could persist over a temperature range of about 20°C and Vs will depend on the geometry of brine pockets (e.g., Dou et al., 2017). Low Vs is possible if the ice is noncementing, and the diagnostic observation would be a high ratio of P wave velocity to Vs, likely >2 (Dou et al., 2017).

The local absence of an ice-saturated cryosphere at the equatorial latitude of the InSight lander would lead to the loss of water from, and drying of, underlying aquifers (Grimm et al., 2017) – if aquifers exist, vapor transport would replenish a cryosphere. Analysis of single-layered ejecta craters suggests that the ice-cemented cryosphere was ~1.3 km thick at the equator during the Hesperian-Amazonian implying that a cryosphere once existed (Weiss & Head, 2017). Ground ice is presently found, and is stable (or more stable), at higher latitudes (e.g., Dundas et al., 2021; Morgan et al., 2021), but water in underlying aquifers confined at high latitudes could be lost through the breach in confinement at low latitudes (Grimm et al., 2017) unless aquifers are laterally compartmentalized (Harrison & Grimm, 2009). The absence of a confining ice-saturated crust at low latitudes thus has global implications for the

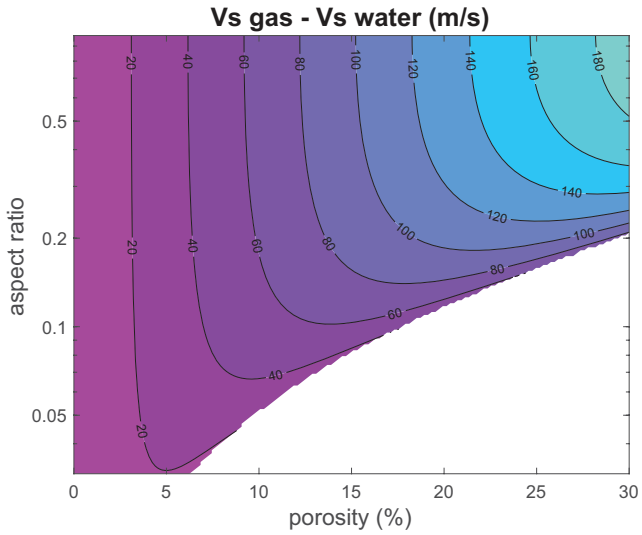

Figure 3. Difference in S wave velocity shear wave velocity (Vs) of gas-filled and liquid water-filled pores (contours in m/s). Vs should decrease upon entering a water-saturated aquifer. Velocity changes from saturating an aquifer are probably too small to detect unless pore geometry and/or porosity also change. White shows regions where the Wu (1966) model leads to unphysical velocities as approximations break down.

present existence deep aquifers. No cryosphere suggests that there are no globally connected aquifers.

4.2. Evidence for an Aquifer

Replacing ice with gas or liquid water in the pores of the upper crust greatly reduces Vs to values that can be lower than 2 km/s (Figure 2). For plausible combinations of pore geometries and porosities, with porosities from 5% to 15% and aspect ratios 0.03 to 0.1, it is possible to obtain the observed upper crustal Vs. For example, Adam and Otheim (2013) used similar rock physics models for Snake River Plain basalt (a reasonable Mars analog) and found that aspect ratios of ~0.02–0.1 fit measured velocities and were similar to pores imaged directly in computed tomography models. A porosity of 10%, for example, implies a dry density of 2,610 kg/m^3 (and water-saturated density of 2,710 kg/m^3), similar to some estimates of the bulk crust density of 2,582 ± 209 kg/m^3 (Goossens et al., 2017). Thus, based on measured velocities, analogue materials, and estimated densities, a gas or liquid-filled crust is most consistent with the InSight measurements.

It is challenging to distinguish between water and gas-filled pores. Since the shear modulus is the same for both fluids, and the bulk density increase from saturating pores with water is small, there is only a relatively small decrease in Vs when transitioning from dry to water-saturated rocks (Figure 3). For properties that lead to Vs < 2 km/s, the change in velocity is usually less than 100 m/s. Velocity reductions <100 m/s are smaller than the uncertainties in velocities and velocity changes. A velocity decrease that might demark the top of an aquifer has not yet been identified or inferred within the crust.

Vs may increase by 0.5–1 km/s at depths between 8 and 11 km owing to decreases in porosity and/or increases in pore aspect ratio, assuming no lithology changes. For illustrative purposes, consider a porosity of 10%, for which an (reasonable) aspect ratio of 0.06 (Adam & Otheim, 2013) leads to a velocity of ~2 km/s for dry or wet rocks, and similar to the Martian upper crust. Slightly less elongated pores (aspect ratio 0.08) will raise the velocity by ~0.5 km/s. Alternatively, decreasing porosity by ~2% would cause the same increase in velocity. Two possible ways of decreasing porosity and/or increasing pore aspect ratios are through cementation and compaction.

Cementation can decrease pore elongation and porosity simultaneously via precipitation of minerals at narrow pore apertures. Sequestering 1 bar of CO_2 as carbonate cement requires 1 weight % cement over a depth range of 2 km (e.g., Kite & Daswani, 2019). Precipitation of carbonate is favored in the deep crust owing to high rock to water ratios (Kissick et al., 2021). Assuming a heat flow of ~18 mW/m^2 (Parro et al., 2017), a thermal conductivity of 2–3 W/mK (Gyalay et al., 2020), and a mean surface temperature of 70 K below freezing and a linear temperature gradient, the melting temperature of ice is reached at a depth of 7.8–11.7 km–with considerable depth uncertainty owing to uncertainty in the heat flow and thermal conductivity. The depth of the velocity increase is similar to the depth at which liquid water would be stable at present and in the past. Depending on the pore geometry and porosity, between about 1 and 5 volume % precipitated carbonates may explain the observed increase in Vs, assuming similar mineral properties for basalt and carbonate cement.

Viscous creep-induced compaction and pore closure can also decrease porosity and increase aspect ratio (less elongated pores) and has been suggested as the cause of the velocity increase (Gyalay et al., 2020). Since compaction has an exponential time dependence and viscosity depends exponentially on temperature, the porosity change has a double exponential dependence on temperature leading to a very sharp and near-complete porosity reduction below some depth. If this were the case, we should expect Vs to increase to ~3.7 km/s (larger than observed) unless subsequent processes such as impacts, tectonics, and thermal stresses created new porosity and fractures.

In the present study, we focus on Vs as a probe of subsurface hydrogeology. InSight offers other opportunities to search for confined aquifers. If fluid pressure in a cryosphere or otherwise confined aquifer is high, the state of stress may be close to that needed to initiate slip on faults, and tidal stresses may trigger marsquakes (Heimisson & Avouac, 2020; Manga et al., 2019). Unfortunately, the large diurnal variations in noise, and hence the ability to detect marsquakes (Giardini et al., 2020), makes it somewhere between very difficult and impossible to identify tidal modulation of seismicity (Knapmeyer et al., 2021).

5. Conclusions

The uncertainties in Vs-depth profiles provide some limitations on quantifying Mars' subsurface hydrogeology, and the values we sought to interpret may become better constrained over the coming years. Assuming that Vs is ∼2 km/s or lower in the upper ∼8–10 km of the crust and there are sharp or gradual Vs increases of ∼0.5–1 km/s at greater depths does, however, allow us to draw some general conclusions. These units are unlikely to be ice-saturated. Hence there cannot be a confining cryosphere above any groundwater unless the layer is thin enough to be (currently) seismically undetectable. Whether or not *unconfined* liquid water aquifers exist cannot be robustly constrained by the published Vs models because the presence of water versus gas has a small effect on Vs. Since evaporation from an aquifer leads to condensation of ice in the overlying crust, the absence of an ice-cemented cryosphere implies no underlying aquifer, at least locally and at present. However, the velocity increase at a depth of 8–11 km could be explained by the presence of a few volume percent of mineral cement such as carbonates precipitated from groundwater, which may be indirect evidence for large volumes of past groundwater.

Data Availability Statement

No data was used in this study.

Acknowledgments
The authors thank the InSight team for their dedication and remarkable accomplishments. M. Manga was supported by NASA grant 80NSSC19K0545. The authors thank the reviewers, J. Ajo-Franklin, S. Clifford, and R. Grimm for constructive comments. The MATLAB script for creating the figures is available at 10.5281/zenodo.4658394.

References

Abotalib, A. Z., & Heggy, E. (2019). A deep groundwater origin for recurring slope lineae on Mars. *Nature Geoscience*, *12*(4), 235–241. https://doi.org/10.1038/s41561-019-0327-5

Adam, L., & Otheim, T. (2013). Elastic laboratory measurements and modeling of saturated basalts. *Journal of Geophysical Research: Solid Earth*, *118*, 840–851. https://doi.org/10.1002/jgrb.50090

Andrews-Hanna, J. C., & Phillips, R. J. (2007). Hydrological modeling of outflow channels and chaos regions on Mars. *Journal of Geophysical Research*, *112*(E8), E08001. https://doi.org/10.1029/2006JE002881

Baker, V. R. (1982). *The channels of Mars* (p. 198). Bristol. Hilger.

Baker, V. R. (2001). Water and the Martian landscape. *Nature*, *412*(6843), 228–236. https://doi.org/10.1038/35084172

Berryman, J. G. (1980). Long-wavelength propagation in composite elastic media II. Ellipsoidal inclusions. *Journal of the Acoustical Society of America*, *68*(6), 1820–1831. https://doi.org/10.1121/1.385172

Burr, D. M., McEwen, A. S., Sakimoto, S. E. H. (2002). Recent aqueous floods from the Cerberus Fossae, Mars. *Geophysical Research Letters*, *29*(1), 13–1. https://doi.org/10.1029/2001gl013345

Carr, M. H. (1979). Formation of Martian flood features by release of water from confined aquifers. *Journal of Geophysical Research*, *84*(B6), 2995–3007. https://doi.org/10.1029/jb084ib06p02995

Carr, M. H., & Carr, M. H. (1996). *Water on Mars*. New York. Oxford University Press.

Citron, R. I., Manga, M., & Hemingway, D. J. (2018). Timing of oceans on Mars from shoreline deformation. *Nature*, *555*(7698), 643–646. https://doi.org/10.1038/nature26144

Clifford, S. M., Lasue, J., Heggy, E., Boisson, J., McGovern, P., & Max, M. D. (2010). Depth of the Martian cryosphere: Revised estimates and implications for the existence and detection of subpermafrost groundwater. *Journal of Geophysical Research*, *115*, E07001. https://doi.org/10.1029/2009JE003462

Clifford, S. M., & Parker, T. J. (2001). The evolution of the Martian hydrosphere: Implications for the fate of a primordial ocean and the current state of the northern plains. *Icarus*, *154*(1), 40–79. https://doi.org/10.1006/icar.2001.6671

Dou, S., Nakagawa, S., Dreger, D., & Ajo-Franklin, J. (2017). An effective-medium model for P-wave velocities of saturated, unconsolidated saline permafrost. *Geophysics*, *82*(3), EN33–EN50. https://doi.org/10.1190/geo2016-0474.1

Dundas, C. M, Mellon, M. T., Conway, S. J., Daubar, J. D., Williams, K. E., Ojha, L., et al. (2021). Widespread exposures of extensive clean shallow ice in the midlatitudes of Mars. *Journal of Geophysical Research: Planets*, *126*, e2020JE006617. https://doi.org/10.1029/2020je006617

Gagnon, R. E., Kiefte, H., Clouter, M. J., & Whalley, E. (1988). Pressure dependence of the elastic constants of ice Ih to 2.8 kbar by Brillouin spectroscopy. *The Journal of Chemical Physics*, *89*(8), 4522–4528. https://doi.org/10.1063/1.454792

Giardini, D., Lognonné, P., Banerdt, W. B., Pike, W. T., Christensen, U., Ceylan, S., et al. (2020). The seismicity of Mars. *Nature Geoscience*, *13*(3), 205–212.

Golombek, M., Warner, N. H., Grant, J. A., Hauber, E., Ansan, V., Weitz, C. M. , et al. (2020). Geology of the InSight landing site on Mars. *Nature Communications*, *11*(1), 1–11.

Goossens, S., Sabaka, T. J., Genova, A., Mazarico, E., Nicholas, J. B., & Neumann, G. A. (2017). Evidence for a low bulk crustal density for Mars from gravity and topography. *Geophysical Research Letters*, *44*, 7686–7694. https://doi.org/10.1002/2017gl074172

Grimm, R. E., Harrison, K. P., Stillman, D. E., & Kirchoff, M. R. (2017). On the secular retention of ground water and ice on Mars. *Journal of Geophysical Research: Planets*, *122*(1), 94–109. https://doi.org/10.1002/2016je005132
Gyalay, S., Nimmo, F., Plesa, A. C., & Wieczorek, M. (2020). Constraints on thermal history of mars from depth of pore closure below InSight. *Geophysical Research Letters*, *47*(16), e2020GL088653. https://doi.org/10.1029/2020gl088653
Harrison, K. P., & Grimm, R. E. (2004). Tharsis recharge: A source of groundwater for Martian outflow channels. *Geophysical Research Letters*, *31*, L14703. https://doi.org/10.1029/2004gl020502
Harrison, K. P., & Grimm, R. E. (2009). Regionally compartmented groundwater flow on Mars. *Journal of Geophysical Research*, *114*, E04004. https://doi.org/10.1029/2008JE003300
Head, J. W., Wilson, L., & Mitchell, K. L. (2003). Generation of recent massive water floods at Cerberus Fossae, Mars by dike emplacement, cryospheric cracking, and confined aquifer groundwater release. *Geophysical Research Letters*, *30*(11), 1577. https://doi.org/10.1029/2003gl017135
Heap, M. J. (2019). P- and S-wave velocity of dry, water-saturated, and frozen basalt: Implications for the interpretation of Martian seismic data. *Icarus*, *330*, 11–15. https://doi.org/10.1016/j.icarus.2019.04.020
Heimisson, E. R., & Avouac, J. P. (2020). Analytical prediction of seismicity rate due to tides and other oscillating stresses. *Geophysical Research Letters*, *47*, e2020GL090827. https://doi.org/10.1029/2020gl090827
Jakosky, B. M. (2021). Atmospheric loss to space and the history of water on Mars. *Annual Review of Earth and Planetary Sciences*, *49*. https://doi.org/10.1146/annurev-earth-062420-052845
Kissick, L. E., Mather, T. A., & Tosca, N. J. (2021). Unravelling surface and subsurface carbon sinks within the early Martian crust. *Earth and Planetary Science Letters*, *557*, 116663. https://doi.org/10.1016/j.epsl.2020.116663
Kite, E. S., & Daswani, M. M. (2019). Geochemistry constrains global hydrology on early Mars. *Earth and Planetary Science Letters*, *524*, 115718. https://doi.org/10.1016/j.epsl.2019.115718
Knapmeyer-Endrun, B., Panning, M. P., Scholz, J. -R., Khan, A., Kim, D., Schmerr, N., et al. (2020). *New seismological constraints on the crustal structure of Mars and the Moon*. AGU asbtract DI026-01.
Knapmeyer, M., Stähler, S. C., Daubar, I., Forget, F., Spiga, A., Pierron, T., et al. (2021). *Marsquake activity driven by the sun?* LPSC abstract 1069.
Lauro, S. E., Pettinelli, E., Caprarelli, G., Guallini, L., Rossi, A. P., Mattei, E., et al. (2021). Multiple subglacial water bodies below the south pole of Mars unveiled by new MARSIS data. *Nature Astronomy*, *5*(1), 63–70. https://doi.org/10.1038/s41550-020-1200-6
Lognonné, P., Banerdt, W. B., Pike, W. T., Giardini, D., Christensen, U., Garcia, R. F., et al. (2020). Constraints on the shallow elastic and anelastic structure of Mars from InSight seismic data. *Nature Geoscience*, *13*(3), 213–220.
Manga, M. (2004). Martian floods at Cerberus Fossae can be produced by groundwater discharge. *Geophysical Research Letters*, *31*, L02702. https://doi.org/10.1029/2003gl018958
Manga, M., Zhai, G., & Wang, C. Y. (2019). Squeezing marsquakes out of groundwater. *Geophysical Research Letters*, *46*, 6333–6340. https://doi.org/10.1029/2019gl082892
Mavko, G., Mukerji, T., & Dvorkin, J. (1998). *The rock physics handbook*. Cambridge university press.
Morgan, G. A., Putzig, N. E., Perry, M. R., Sizemore, H. G., Bramson, A. M., Petersen, E. I., et al. (2021). Availability of subsurface water-ice resources in the northern mid-latitudes of Mars. *Nature Astronomy*, 1–7.
Ojha, L., Karimi, S., Buffo, J., Nerozzi, S., Holt, J. W., Smrekar, S., & Chevrier, V. (2021). Martian mantle heat flow estimate from the lack of lithospheric flexure in the south pole of Mars: Implications for planetary evolution and basal melting. *Geophysical Research Letters*, *48*, e2020GL091409. https://doi.org/10.1029/2020gl091409
Orosei, R., Lauro, S. E., Pettinelli, E., Cicchetti, A., Coradini, M., Cosciotti, B., et al. (2018). Radar evidence of subglacial liquid water on Mars. *Science*, *361*(6401), 490–493.
Parro, L. M., Jiménez-Díaz, A., Mansilla, F., & Ruiz, J. (2017). Present-day heat flow model of Mars. *Scientific Reports*, *7*(1), 1–9. https://doi.org/10.1038/srep45629
Rodriguez, J. A. P., Kargel, J. S., Baker, V. R., Gulick, V. C., Berman, D. C., Fairén, A. G. , et al. (2015). Martian outflow channels: How did their source aquifers form and why did they drain so rapidly?. *Scientific Reports*, *5*(1), 1–10. https://doi.org/10.1038/srep15092
Scheller, E. L., Ehlmann, B. L., Hu, R., Adams, D. J., & Yung, Y. L. (2021). Long-term drying of Mars by sequestration of ocean-scale volumes of water in the crust. *Science*, *372*, 56–62. https://doi.org/10.1126/science.abc7717
Sori, M. M., & Bramson, A. M. (2019). Water on Mars, with a grain of salt: Local heat anomalies are required for basal melting of ice at the south pole today. *Geophysical Research Letters*, *46*, 1222–1231. https://doi.org/10.1029/2018gl080985
Tanaka, K. L. (1997). Sedimentary history and mass flow structures of Chryse and Acidalia Planitiae, Mars. *Journal of Geophysical Research*, *102*(E2), 4131–4149. https://doi.org/10.1029/96je02862
Voigt, J. R. C., & Hamilton, C. W. (2018). Investigating the volcanic versus aqueous origin of the surficial deposits in Eastern Elysium Planitia, Mars. *Icarus*, *309*, 389–410. https://doi.org/10.1016/j.icarus.2018.03.009
Wang, C. Y., Manga, M., & Hanna, J. C. (2006). Can freezing cause floods on Mars? *Geophysical Research Letters*, *33*, L20202. https://doi.org/10.1029/2006gl027471
Weiss, D. K., & Head, J. W. (2017). Evidence for stabilization of the ice-cemented cryosphere in earlier Martian history: Implications for the current abundance of groundwater at depth on Mars. *Icarus*, *288*, 120–147. https://doi.org/10.1016/j.icarus.2017.01.018
Wu, T. T. (1966). The effect of inclusion shape on the elastic moduli of a two-phase material. *International Journal of Solids and Structures*, *2*(1), 1–8. https://doi.org/10.1016/0020-7683(66)90002-3